View metadata, citation and similar papers at core.ac.uk

brought to you by CORE

provided by Edinburgh Research Explorer

THE UNIVERSITY of EDINBURGH

Edinburgh Research Explorer

Direct top-down fabrication of nanoscale electrodes for organic semiconductors using fluoropolymer resists

Citation for published version:
Park, J, Ho, J, Yun, H, Park, M, Lee, JH, Seo, M, Campbell, EEB, Lee, C, Pyo, S & Lee, S 2013, 'Direct top-down fabrication of nanoscale electrodes for organic semiconductors using fluoropolymer resists' Applied Physics A: Materials Science & Processing, vol. 111, no. 4, pp. 1051-1056. DOI: 10.1007/s00339-012-7411-7

Digital Object Identifier (DOI):
10.1007/s00339-012-7411-7

Link:
Link to publication record in Edinburgh Research Explorer

Document Version:
Peer reviewed version

Published In:
Applied Physics A: Materials Science & Processing

Publisher Rights Statement:
Copyright © 2012 Springer-Verlag Berlin Heidelberg. All rights reserved.

General rights
Copyright for the publications made accessible via the Edinburgh Research Explorer is retained by the author(s) and / or other copyright owners and it is a condition of accessing these publications that users recognise and abide by the legal requirements associated with these rights.

Take down policy
The University of Edinburgh has made every reasonable effort to ensure that Edinburgh Research Explorer content complies with UK legislation. If you believe that the public display of this file breaches copyright please contact openaccess@ed.ac.uk providing details, and we will remove access to the work immediately and investigate your claim.

Download date: 05. Apr. 2019

Post-print of peer-reviewed article published by Springer.
The final publication is available at: http://dx.doi.org/10.1007/s00339-012-7411-7

Cite as:
Park, J., Ho, J., Yun, H., Park, M., Lee, J. H., Seo, M., Campbell, E., Lee, C., Pyo, S., & Lee, S. (2013). Direct top-down fabrication of nanoscale electrodes for organic semiconductors using fluoropolymer resists. *Applied Physics A: Materials Science & Processing*, 111(4), 1051-1056.

Manuscript received: 28/07/2012; Accepted: 29/10/2012; Article published: 16/11/2012

Direct top–down fabrication of nanoscale electrodes for organic semiconductors using fluoropolymer resists**

Jungho Park,[1,‡] Jonathan Ho,[1,2,‡] Hoyeol Yun,[1] Myeongjin Park,[3] Jung Hyun Lee,[4] Miri Seo,[1] Eleanor E. B. Campbell,[1,2] Changhee Lee,[3] Seungmoon Pyo[4] and Sang Wook Lee[1,*]

[1]Division of Quantum Phases and Devices, School of Physics, Konkuk University, Seoul, 143-701, Korea.

[2]EaStCHEM, School of Chemistry, Joseph Black Building, University of Edinburgh, West Mains Road, Edinburgh, EH9 3JJ, UK.

[3]School of Electrical Engineering, Seoul National University, Seoul, 151-744, Korea.

[4]Department of Chemistry, Konkuk University, Seoul, 143-701, Korea.

[‡]These authors contributed equally to this work.

[*]Corresponding author; e-mail: leesw@konkuk.ac.kr

[**]This work was supported through BSR (2011-0021207), WCU (R31-2008-000-10057-0), and framework of international cooperation programs by the National Research Foundation of Korea (NRF) funded by the Ministry of Education, Science and Technology.

Keywords:
Nanolithography, organic electronics, top-contact

Abstract

We report the use of a fluoropolymer resist for the damage-free e-beam lithographic patterning of organic semiconductors. The same material is also shown to be suitable as an orthogonal electron beam resist for the patterning of top-contact electrodes on organic thin films. We demonstrate this by characterizing pentacene field effect transistors with feature sizes as small as 100 nm and compare the performance of bottom- and top-contacted devices.

1. Introduction

Organic electronic devices are a rapidly developing alternative to silicon-based electronics because of their inherent advantages such as low cost, printability, and flexibility.[1-4] In recent decades, organic electronic devices such as light emitting diodes, thin film transistors, and solar cells have advanced dramatically in performance and are on the verge of commercialization for a wide range of applications.[5-8]As for silicon devices, there are advantages in downscaling the channel size of organic transistors in order to improve performance and to study the scaling properties to understand the transport characteristics and maximize device performance. Although accurate and scalable photo- and electron beam lithography has been used in silicon processing for many years to make structures on the nanoscale, the technique has been of limited use for the realization of organic electronic devices, which are chemically incompatible with the resists and solvents traditionally used.

Several strategies have been developed for patterning of organic electronic devicesincluding inkjet printing, transfer printing, imprint lithography, shadow mask deposition, orthogonal processing, and interlayer photolithography.[9-21] Photolithography remains the most attractive thin film patterning technique to date due to its compatibility with industrial large-scale processing and its relative simplicity. In interlayer photolithography, inert protective inter-layers are inserted between the photoresist layer and the functional organic layer to be patterned. After photolithographic patterning is carried out in the conventional manner, the photoresist layer and interlayer are separated from the active layer. The manner in which these layers are removed depends on the type of interlayer, e.g., parylene C layers can be physically peeled off the active layer, while fluoropolymer layers are dissolved in fluorinated solvents, which are orthogonal to all other non-fluorinated polymers [21]. Standard photolithography is, however, limited to structures with resolution greater than 100 nm. Here, we investigate the use of electron-beam lithography, the most common technique used to produce nanoscale devices, for patterning organic layers and depositing top-contact nanoscale electrodes. Following the successful photolithography strategies, we make use of a fluoropolymer as the protective interlayer resist that is deposited on top of the active organic layer. A feature size smaller than 100 nm can be achieved in the patterning process if the fluoropolymer is combined with a commercially available e-beam resist. As a proof-of-concept, we fabricated hole-only pentacene devices with channel lengths ranging from

100 nm to 500 nm and characterised their charge carrier mobilities. We show that the top-contacted devices made possible using our approach consistently show higher mobility than otherwise identical bottom-contacted devices. This is a consequence of the improved carrier injection, smaller contact resistance and better organic film quality obtainable with top-contacted devices.

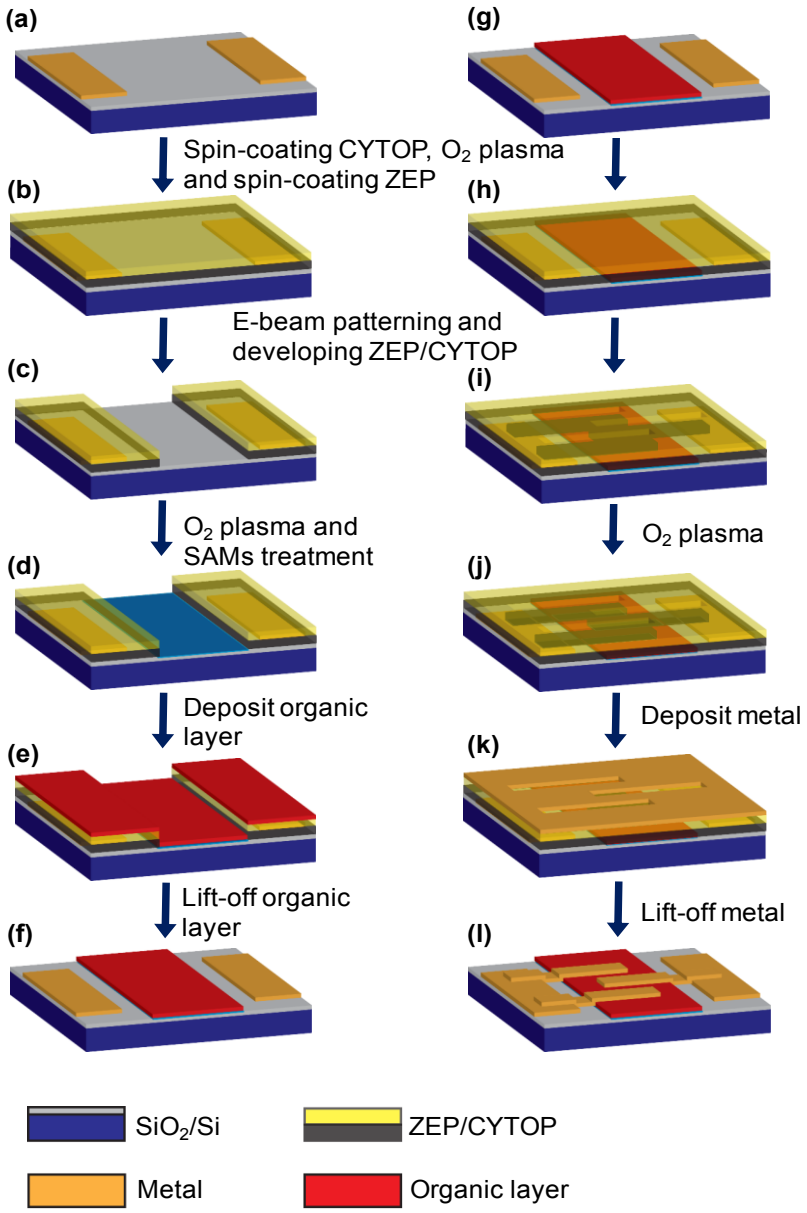

Figure 1. Schematics of pentacene nano electronic device fabrication procedure for top electrode configuration. (a) Microscale metal electrode was pre-defined on a Si/SiO_2 substrate. (b) CYTOP layer was spin-coated and O_2 plasma was applied before the ZEP layer was spin coated on top of CYTOP. (c) Pentacene pattern area was exposed by electron beam lithography followed by development process. (d) Self assembled monolayer was deposited to improve the crystalline structure of pentacene. (e) (f) Organic layer pattern was prepared after pentacene evaporation followed by lift-off process. (g) (h) ZEP/CYTOP double layer was

immediately spin coated on top of the patterned organic layer to avoid possible degradation. (i) Nanoscale electrode patterns were exposed by electron beam lithography and developed. (j) O_2 plasma treatment was applied to remove residues. (k) (l) The device fabrication was completed after Au evaporation and following lift-off process.

2. Device Fabrication

The patterning procedure is outlined schematically in Fig. 1. The key to this approach is the use of a fluoropolymer that is soluble only in fluorinated solvents, which are highly orthogonal to all other solvents for most organic semiconductors. Moreover, after patterning, the fluoropolymer needs to be removed without leaving any residues and without degrading the surface of the organic semiconductor. It has been shown that a fluoropolymer CYTOP (Asahi Glass Co.) meets these requirements. CYTOP has been used as a low-k gate dielectric in organic FETs and as a protective interlayer for the underlying organic semiconductors in conventional photolithography.[20-26] In this study, we investigated the possibility of using CYTOP as an e-beam resist. CYTOP solution with a concentration of 9 wt% was purchased. The original solution was diluted with a fluorinated solvent FC-40 (3M Co.) to obtain a final solution with a CYTOP:FC-40 ratio of 4:1 (by wt). The diluted CYTOP solution was spin-coated onto a SiO_2/Si wafer in a main spin cycle at 1800 rpm for 45 s and subsequently baked at 150 °C for 2 min to obtain a film thickness of ~200 nm. Using a modified SEM (Tescan VEGA TS 5130MM) equipped with an electron beam lithography system (Elphy Quantum, Raith GmbH), the patterning conditions for the CYTOP films were investigated. CYTOP (4:1 CYTOP:FC-40) was successfully patterned using an electron beam energy of 30 keV and a beam current of 20 pA at a dose of 100 $\mu C/cm^2$ and developed in FC-40 for 30 s. However, the edge profiles of CYTOP patterns were still not fully sufficient for lift-off at the nanoscale level. When working with the e-beam resist ZEP520 (ZEON Co.), hereafter referred to as ZEP, 100-nm patterns could be obtained without extensive optimization, which suggests that lithography in which a ZEP/CYTOP double layer is employed can be a useful tool for realizing sub-100-nm features. A 1:1 mixture of ZEP520:anisol by weight was initially prepared to spin-cast 100-nm-thick layers at 4500 rpm for 2 min. However, the orthogonality of CYTOP made this difficult. Since, the organic ZEP and the fluoropolymer CYTOP were designed to be immiscible and non-interacting, all attempts to spin-coat ZEP on CYTOP were unsuccessful. Conversely, coating CYTOP on organic materials was easy; and it was achieved using standard spin-coating conditions similar to those used for coating on SiO_2. ZEP could be successfully spin-coated on a CYTOP film that was first treated with O_2 plasma (20 sccm, 20 mTorr, 50 W, 10 s). The ZEP layer could then be patterned using the same exposure conditions as those for CYTOP (30 keV, 20 pA, 100 $\mu C/cm^2$); ZEP development was carried out in hexyl acetate for 2 min and CYTOP development was carried out in FC-40 for 30 s. Once again, O_2 plasma was used (20 sccm, 20 mTorr, 100 W, 15 s) and its use proved to be effective at etching away the undeveloped CYTOP residue.

In order to improve the crystalline structure of the first few organic layers that are critical for charge mobility of bottom-contacted devices, self-assembled monolayers (SAMs), hexamethyldisilazane (HMDS) oroctadecyltrichlorosilane (OTS), were deposited on the SiO_2 surface before the active organic layer was deposited. For the same reason, pentafluorobenzenethiol (PFBT) was deposited on the surface of the Au electrodes [27, 28] The SAM chemicals were purchased from Aldrich Chemical Co. Prior to SAM formation, the substrates were exposed to O_2 plasma for 2 min. For HMDS treatment, HMDS solution was spin-coated onto a SiO_2/Si wafer at 4500 rpm for 2 min and subsequently baked at 180 °C for 2 min. For OTS treatment, the substrates were dipped into a 2 mM OTS solution, dissolved in hexadecane by stirring for 30 min to form a hydrophobic surface, and cleaned in an ultrasonic bath for 10 min each with chloroform, isopropyl alcohol, and methanol. A SAM of PFBT was formed on the Au electrodes by immersing the electrodes for 15 min in a 10 mM solution of PFBT in ethanol and subsequent rinsing with ethanol.

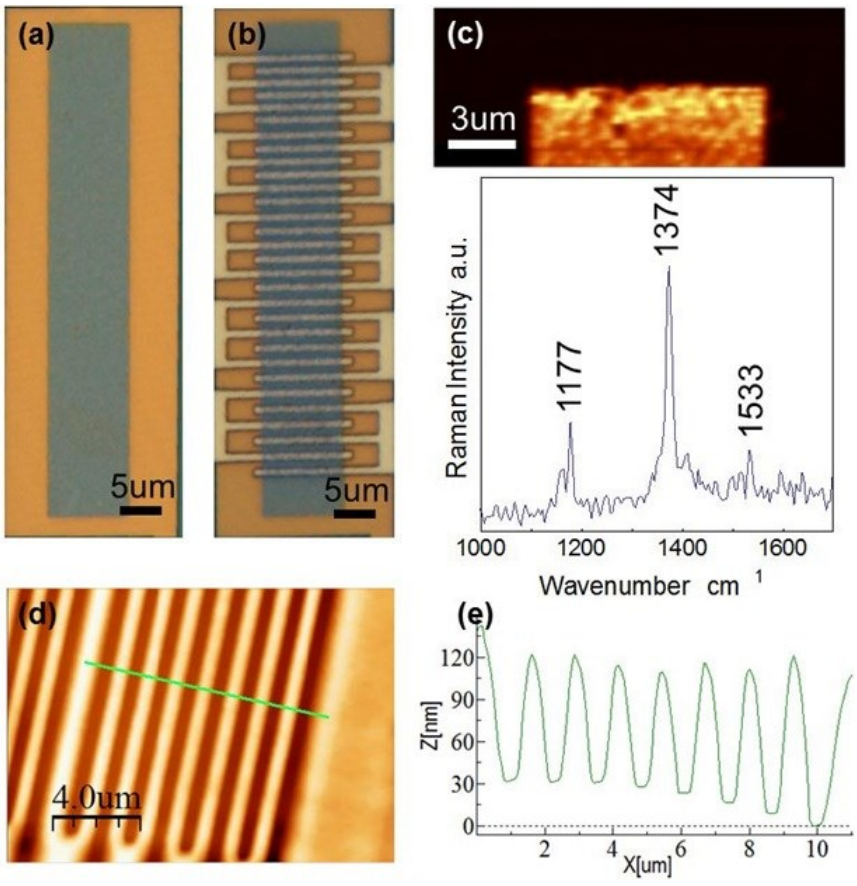

Figure 2.Optical micrographs of (a) a 10 × 60 μm^2 area of pentacene and (b) an array of top-contact interdigitated Au electrodes. (c) 2D Raman image showing the intensity of a characteristic C–C aromatic stretching band at 1374 cm^{-1}at the top edge of the pentacene area shown in (a) and a typical Raman spectrum from the patterned pentacene active area. (d) A tapping-mode AFM surface topography image and (e) the AFM cross section of the interlocked electrode structure patterned in the CYTOP pattern.

The lift-off patterning leads to the formation of organic or metal layers of the designed pattern when a positive-tone ZEP/CYTOP resist is used. Here, pentacene was used as the active organic semiconductor because it has one of the highest hole mobilities (up to 1 cm^2/Vs) for a polycrystalline film and moderate stability to O_2 and light.[29, 30] However, because of the degradation in an O_2-rich atmosphere, the whole device was covered with an additional layer of CYTOP immediately after deposition. It has been demonstrated (Fig. 2) that the pentacene active area and the CYTOP layer could be patterned using e-beam exposure. The deposition of a pentacene film and the following lift-off of the film led to the formation of an active area pattern (Fig. 2(a)). A pentacene film with a thickness of ~30 nm was deposited via thermal evaporation at a rate of 0.3 Å/s on the substrates that were pretreated with the two different types of SAMs. After the secondary deposition of ZEP/CYTOP and electrode patterning (Fig. 2(d), (e)), a Au (50 nm) layer was deposited via e-beam evaporation to form interdigitated Au electrodes on the active area (Fig. 2(b)). Fig. 2(c) shows a 2D Raman image of a characteristic aromatic C–C stretching band at 1374 cm^{-1} obtained using an alpha300R confocal Raman microscope (WITec), indicating the presence of the patterned pentacene active area. The Raman spectrum measured over the range 1000 cm^{-1} to 1700 cm^{-1} shows characteristic bands attributed to C–H in-plane bending at 1177 cm^{-1}, C–C aromatic stretching at 1374 cm^{-1}, and C–C in-plane stretching at 1533 cm^{-1}.[31, 32] Lift-off was performed in hot PF-5060 (3M Co.) for over 6 h. Fig. 2(d) shows the AFM micrograph of the patterned CYTOP in FC-40, which was examined by using a Nanoscope IV (Digital Instruments). The cross section of the AFM micrograph (Fig. 2(e)) revealed well-defined edges of the desired interlocked finger structure.

3. Device Characterisation

Fig. 3(a) and (b) shows an optical microscope and scanning electron microscope image of the top-contact hole-only pentacene devices with active lengths ranging from 500 nm to 100 nm. Inset of Fig. (a) shows a schematic of the top-contact device geometry. Fig. 3 (c) to (g) shows the zoom-in image of the channel lengths which were designed from 500 nm down to 100 nm. The devices with the top-contact (TC) and bottom-contact (BC) configurations were prepared on SiO_2 surfaces modified by HMDS or OTS (acting as dielectric materials) and PFBT-coated Au electrodes were used for the BC geometry To determine whether the device geometry is influencing the transport properties, the I-V characteristics of the devices with TC and BC geometries were compared. Electrical measurements were carried out by using a point probe station and an Agilent 4155B semiconductor parameter analyzer under ambient conditions. From the back gate voltage dependence of current-voltage (I-V) characteristics, no saturation behavior was observed but the I-V curves follow a power law in voltage as the bias voltage is varied from 0V to -8V. It is likely that current injection, originated by drain-induced barrier lowering (DIBL), could easily happen when the channel length is reduced down to the submicron scale. A gate voltage dependence could not be effectively observed since we have used doped Si as a gate electrode with a SiO_2 dielectric layer.

As shown in Fig. 4(a), most of the TC devices showed an approximate dependence on V^2 at biased voltages beyond 1-2 V, which is an indication of a trap-free space-charge limited current (SCLC), for which the current density is given by the Mott-Gurney law[33]:

$$J = \frac{9}{8}\varepsilon_r \varepsilon_0 \mu_{SCLC} \frac{V^2}{L^3} \qquad (1)$$

where J is the current density,ε_r is the relative dielectric constant of the pentacene film; ε_0, the dielectric constant; μ_{SCLC}, the SCLC mobility; V, the applied voltage; and L, the channel length.

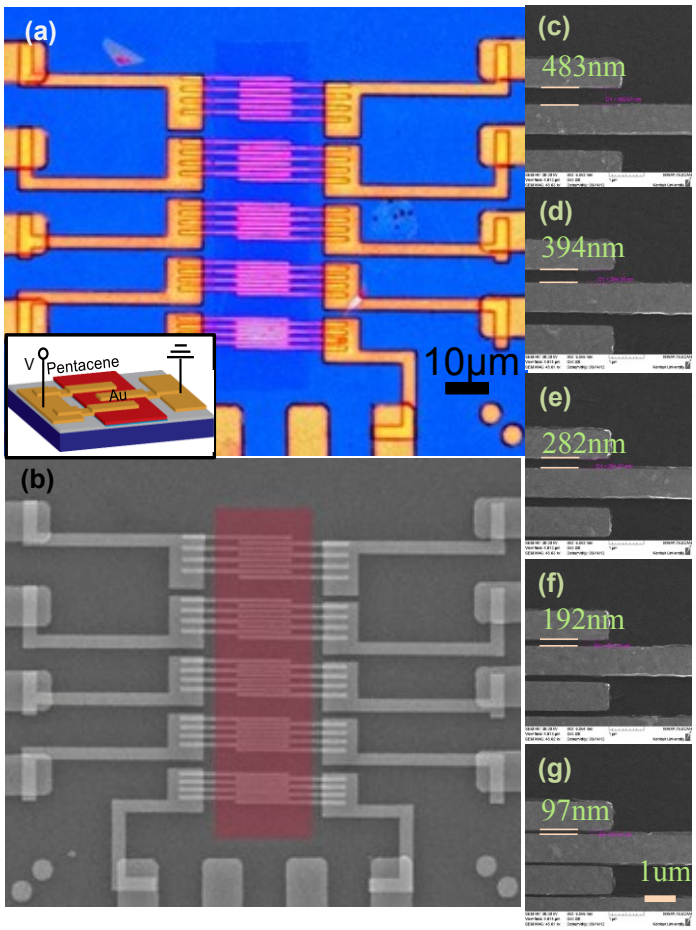

Figure 3. The optical micrograph image (a) and corresponding SEM image (b) of a device consisting of a patterned pentacene active area and an array of top-contact interdigitated Au electrodes on a SAM-treated SiO_2/Si substrate. The channel lengths ranged from 500 nm to 100 nm. (The colour of the patterned pentacene area was modified in (b) because of weak distinction from the bare SEM image.) Inset of (a) shows the

schematic of hole-only pentacene device, along with bias configuration. (c)-(g) Zoom-in images of source-drain electrode with channel lengths from 500 nm down to 100 nm.

The SCLS-hole mobility is extracted from the *I-V* plots in Fig. 4(a) using eq. (1). The results are plotted in Fig. 4(b) as a function of channel length.

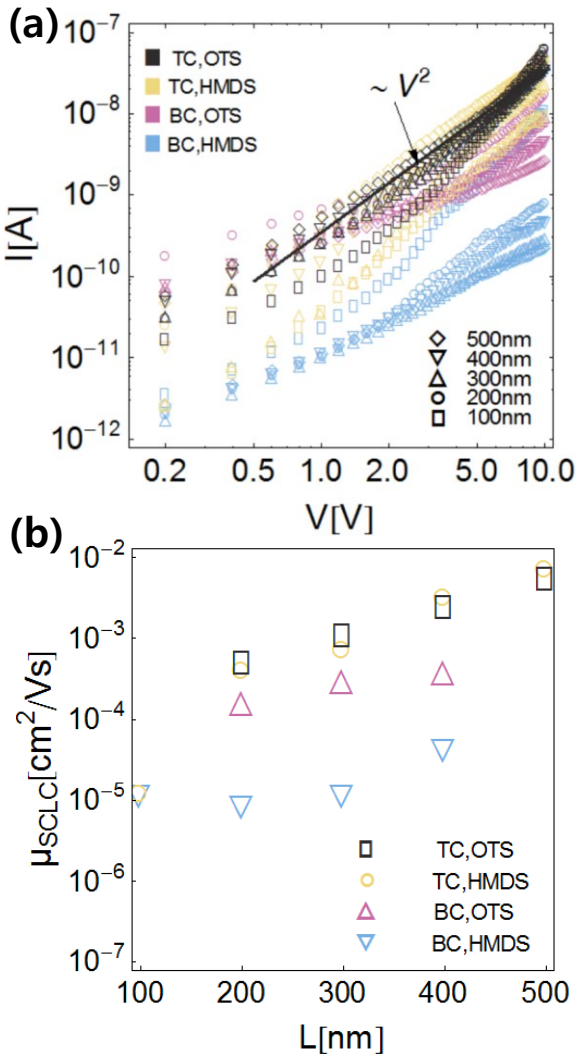

Figure 4. (a) *I-V* characteristics of the devices with TC and BC geometries after modification by various SAMs. The solid line is fitted to the experimental data in accordance with the power law of V^2, appropriate for the regime of space-charge-limited current (SCLC). (b) SCLC-hole mobility of the polycrystalline pentacene films.

Assuming the relative dielectric constant of pentacene to be 3.0 and the thickness of the pentacene film to be 30 nm, the SCLC mobility of the top-contacted devices is seen to lie in the range 0.0001 - 0.01 cm^2/Vs, as shown in Fig. 4(b). It is known that, generally in the case of microscale channel devices, the hole mobilities of polycrystalline pentacene are reported to lie between ca. 10^{-1} to 10^{-3} cm^2/Vs in the case of top contact configurations[34]. The estimated mobility values of our devices in top contact configurations have the same order of magnitude as previously reported for longer channel devices (L = 400 nm and 500 nm). In the case of shorter channels (L = 100 nm – 300 nm), however, the mobility values were estimated to be lower. As one would expect, the values extracted for the top-contacted devices are independent of the type of SAM layer underneath the pentacene. The value extracted for the shortest channel length is significantly lower. This is likely to be due to the increased importance of contact effects. The resistance of the channel decreases as the channel length decreases. Therefore the relative voltage drop across the channel is reduced while the voltage drop from the contact becomes more significant especially in the short channel configuration. This may lead to the observed lowering of the mobility. The BC devices show a significantly lower mobility with the OTS coated substrate performing better than the HMDS substrate.

4. Conclusions

In conclusion, we have developed a simple, versatile, high-resolution lift-off patterning technique that can be used for sub-micrometer patterning of organic semiconductor active layers for applications in light-emitting diodes, thin-film transistors, and solar cells without material degradation. E-beam lithographically patterned sub-microstructures such as hole-only devices with widths as low as 100 nm have been realized. To-date, there have been no reports on the use of CYTOP other than as a dielectric or an interlayer; however, we have shown the potential use of CYTOP as an e-beam resist in this study.

References

[1] S. R. Forrest, Nature, 2004, **428**, 911

[2] H. Sirringhaus, T. Kawase, R. H. Friend, T. Shimoda, M. Inbasekaran, W. Wu, E. P. Woo, Science, 2000, **290**, 2123

[3] G. Gustafsson, Y. Cao, G. M. Treacy, F. Klavetter, N. Colaneri, A. J. Heeger, Nature, 1992, **357**, 477

[4] J. A. Rogers, Z. Bao, Journal of Polymer Science Part A: Polymer Chemistry, 2002, **40**, 3327

[5] J. Y. Lee, J. H. Kwon, H. K. Chung, Organic Electronics, 2003,**4**, 143

[6] S. Reineke, F. Lindner, G. Schwartz, N. Seidler, K. Walzer, B. Lüssem, K. Leo, Nature, 2009,**459**, 234

[7] D. Tobjörk, R. Österbacka, Advanced Materials, 2011,**23**, 1935

[8] R. Gaudiana, C. Brabec, Nature Photonics, 2008, **2**, 287

[9] E. Menard, M. A. Meitl, Y. Sun, J.-U.Park, D. J.-L.Shir, Y.-S. Nam, S. Jeon, J. A. Rogers, Chemical Reviews, 2007,**107**, 1117

[10] L. Jiang, X. Wang, L. Chi, Small, 2011,**7**, 1309

[11] Y. Xu, F. Zhang, X. Feng, Small, 2011, **7**, 1338

[12] Y.-Y. Noh, N. Zhao, M. Caironi, H. Sirringhaus, Nature Nanotechnology, 2007,**2**, 784

[13] S.-H. Hur, D.-Y.Khang, C. Kocabas, J. A. Rogers, Appl. Phys.Lett., 2004,**85**, 5730

[14] M. D. Austin, S. Y. Chou, Appl. Phys.Lett., 2002,**81**, 4431

[15] J. K. Lee, M. Chatzichristidi, A. A. Zakhidov, P. G. Taylor, J. A. DeFranco, H. S. Hwang, H. H. Fong, A. B. Holmes, G. G. Malliaras, C. K. Ober, J. Am. Chem. Soc., 2008,**130**, 11564

[16] A. A. Zakhidov, J.-K. Lee, J. A. DeFranco, H. H. Fong, P. G. Taylor, M. Chatzichristidi, C. K. Ober, G. G. Malliaras, Chemical Science, 2011,**2**, 1178

[17] I. Kymissis, C. D. Dimitrakopoulos, S. Purushothaman, Journal of Vacuum Science and Technology B: Microelectronics and Nanometer Structures, 2002,**20**, 956

[18] I. Kymissis, A. I. Akinwande, V. Bulovic, Journal of Display Technology, 2005,**1**, 289

[19] J. Huang, R. Xia, Y. Kim, X. Wang, J. Dane, O. Hofmann, A. Mosley, A. J. de Mello, J. C. de Mello, D. D. C. Bradley, Journal of Materials Chemistry, 2007,**17**, 1043

[20] J.-F. Chang, M. C. Gwinner, M. Caironi, T. Sakanoue, H. Sirringhaus, Advanced Functional Materials, 2010,**20**, 2825

[21] B. M. Dhar, G. S. Kini, G. Xia, B. J. Jung, N. Markovic, H. E. Katz, Proceedings of the National Academy of Sciences of the United States of America, 2010,**107**, 3972

[22] W. L. Kalb, T. Mathis, S. Haas, a. F. Stassen, B. Batlogg, Appl. Phys.Lett., 2007,**90**, 092104

[23] M. P. Walser, W. L. Kalb, T. Mathis, T. J. Brenner, B. Batlogg, Appl. Phys.Lett., 2009,**94**, 053303

[24] X. Cheng, M. Caironi, Y.-Y. Noh, J. Wang, C. Newman, H. Yan, A. Facchetti, H. Sirringhaus, Chemistry of Materials, 2010,**22,** 1559

[25] T. Sakanoue, H. Sirringhaus, Nature Materials, 2010,**9,** 736

[26] D. K. Hwang, C. Fuentes-Hernandez, J. Kim, W. J. Potscavage, S.-J. Kim, B. Kippelen, Advanced Materials, 2011, **23**, 1293

[27] H. Yang, T. J. Shin, M.-M. Ling, K. Cho, C. Y. Ryu, Z. Bao, Journal of the American Chemical Society, 2005,**127**, 11542

[28] D. J. Gundlach, J. E. Royer, S. K. Park, S. Subramanian, O. D. Jurchescu, B. H. Hamadani, a. J. Moad, R. J. Kline, L. C. Teague, O. Kirillov, C. a. Richter, J. G. Kushmerick, L. J. Richter, S. R. Parkin, T. N. Jackson, J. E. Anthony, Nature Materials, 2008,**7**, 216

[29] R. Matsubara, N. Ohashi, M. Sakai, K. Kudo, M. Nakamura, Applied Physics Letters, 2008**,92**, 242108

[30] C. R. Kagan, a. Afzali, T. O. Graham, Applied Physics Letters, 2005,**86**, 193505

[31] H.-L. Cheng, Y.-S.Mai, W.-Y.Chou, L.-R. Chang, Applied Physics Letters, 2007,**90,** 171926

[32] O. Kwon, V. Coropceanu, N. E. Gruhn, J. C. Durivage, J. G. Laquindanum, H. E. Katz, J. Cornil, J. L. Bredas, The Journal of Chemical Physics, 2004,**120**, 8186

[33] B. Lucas, A. El Amrani, A. Moliton, A. Skaiky, A. El Hajj, M. Aldissi, Solid-State Electronics 2012,**69,**99

[34] D. Gupta, M. Katiyar, D. Gupta, Organic Electronics 2009, **10**, 775